Genitourinary System

7

Mohammad Ghanem
and Abdelhamid H. Elgazzar

7.1 Anatomic and Physiologic Considerations

7.1.1 Major Structures

The urinary system consists of a pair of kidneys, which filters the blood, form urine, and help regulate various metabolic processes; a pair of tubular ureters, which transport urine away from the kidneys; a saclike urinary bladder, which serves as urine reservoir; and a tubular urethra, which conveys urine to the outside of the body.

Kidneys are paired bean-shaped retroperitoneal organs situated in the posterior part of the abdomen on each side of the vertebral column against the psoas major muscle. The upper pole of each kidney lies at the level of the twelfth thoracic vertebra, and the lower pole lies opposite the third lumbar vertebra. The right kidney is usually slightly more caudal in position. Each kidney's weight ranges from 120 g to 170 g in the adult male and from 115 g to 155 g in the adult female. It is approximately 11 × 6 × 2.5 cm in dimension. Each kidney's concave medial surface has a slit-like aperture called the hilum, through which the renal pelvis, the renal artery, and vein, the lymphatics, and a nerve plexus pass into the kidney. A tough fibrous capsule surrounds the organ.

On cut sections, two distinct regions can be identified: a pale outer region, the cortex, and a darker inner region, the medulla. In humans, the medulla is divided into 4–18 striated conical masses, the renal pyramids (average 8). Each pyramid's base is positioned at the corticomedullary boundary, and the apex extends toward the renal pelvis to form a papilla. On the tip of each papilla are 10–25 small openings representing the distal ends of the collecting ducts. A funnel-shaped minor calyx caps the apex of each medullary pyramid. The minor calyx receives the urine from the kidney and passes it to the extrarenal collecting system (Fig. 7.1).

Since renal blood flow of approximately 400 mL/100 g to 1.0 and 1.2 L/min per 1.73 m^2 of body surface area—is much higher than that of any other well-perfused organs such as the heart and brain, kidney tissue is prone to be exposed to a significant amount of any potentially harmful circulating substances [1].

Additionally, glomerular capillaries vulnerable to hemodynamic injury, in contrast to other capillary beds because glomerular filtration is dependent on high intra- and trans-glomerular pressure. The nephron's microvasculature organization facilitates the spreading of glomerular injury to the tubulointerstitial compartment in disease, exposing tubular epithelial cells to abnormal ultrafiltrate. Accordingly, the concept

M. Ghanem (✉) · A. H. Elgazzar
Department of Nuclear Medicine, Faculty of Medicine, Kuwait University, Kuwait City, Kuwait
e-mail: mohammad.sghanem@ku.edu.kw

A. H. Elgazzar (ed.), *The Pathophysiologic Basis of Nuclear Medicine*,
https://doi.org/10.1007/978-3-030-96252-4_7

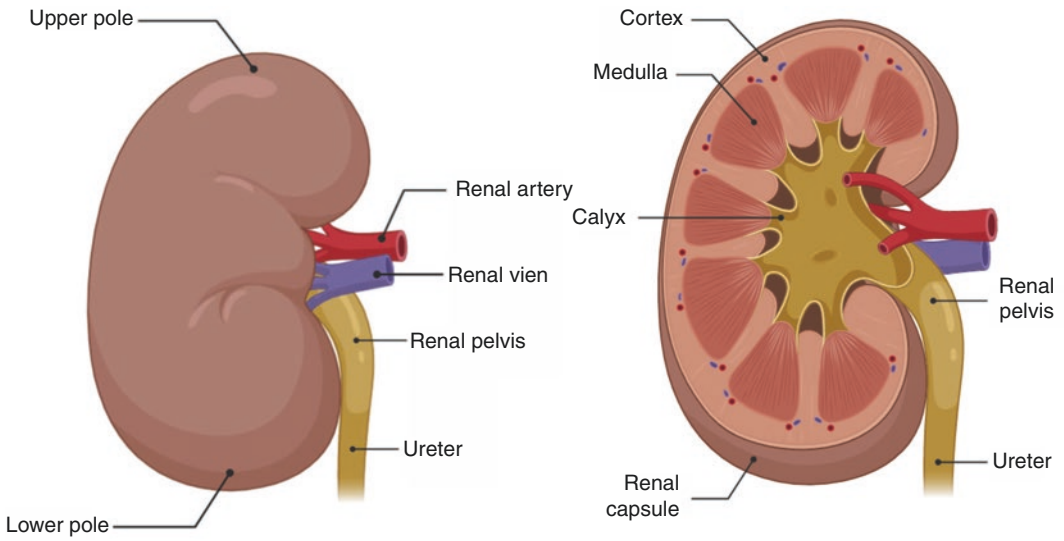

Fig. 7.1 A diagram illustrating main surface renal anatomy. (Created with BioRender.com)

of the nephron as a functional unit applies not only to renal physiology but also to the pathophysiology of renal diseases.

7.1.2 The Nephron

The main functions of the kidneys are the maintenance of water, electrolyte, acid-base balance, elimination of waste products, and blood pressure regulation. The functional unit of the kidney is the nephron, which consists of a glomerulus and a tubule. The *glomerulus* consists of a network of capillaries derived from the afferent glomerular arteriole. They can be broadly divided into several portions: the proximal tubule, loop of Henle, distal tubule, and collecting tubule (Fig. 7.2).

Urine is formed as a result of glomerular filtration, tubular reabsorption, and tubular secretion [2]. The glomerular capillary tuft acts as a filter for plasma. Two epithelial layers encase it, the inner layer becoming part of the outer capillary wall and the outer layer lining Bowman's space (capsule), which receives the filtered fluid. The glomerular filtration rate (GFR) mainly depends on the hydrostatic and colloid osmotic pressure in the glomerular capillaries and the hydrostatic pressure in Bowman's space. Filtered fluid from Bowman's space enters the *tubule*. The *proximal tubule* plays a crucial role in reabsorbing filtered solutes. About half to two-thirds of the sodium, chloride, and potassium are reabsorbed in this segment. Reabsorption of solutes is accompanied by passive osmotic diffusion of water. The *loop of Henle*, consisting of a descending limb and an ascending limb, is the reabsorption site of about 25% of the filtered solutes. Reabsorption occurs primarily in the "thick" ascending limb, where the epithelial cells are thick and metabolically very active. In this section, "loop" diuretics such as furosemide exert their effects (see later). The reabsorbed solutes enter the medullary interstitium and contribute to its hypertonicity.

The *distal tubule* transports sodium, chloride, and potassium, but not water, from its proximal part, similar to the loop of Henle. The terminal distal tubule shares similar functions with the collecting tubules (see later). At the very beginning of the distal tubule is the *macula densa*, a region of specialized cells in the vicinity of the juxtaglomerular (JG) cells in the afferent arteriole that store renin. In response to sodium and chloride concentration changes in this portion of the tubule, the macula densa sends signals to the JG cells to release renin that mainly increases arterial blood pressure.

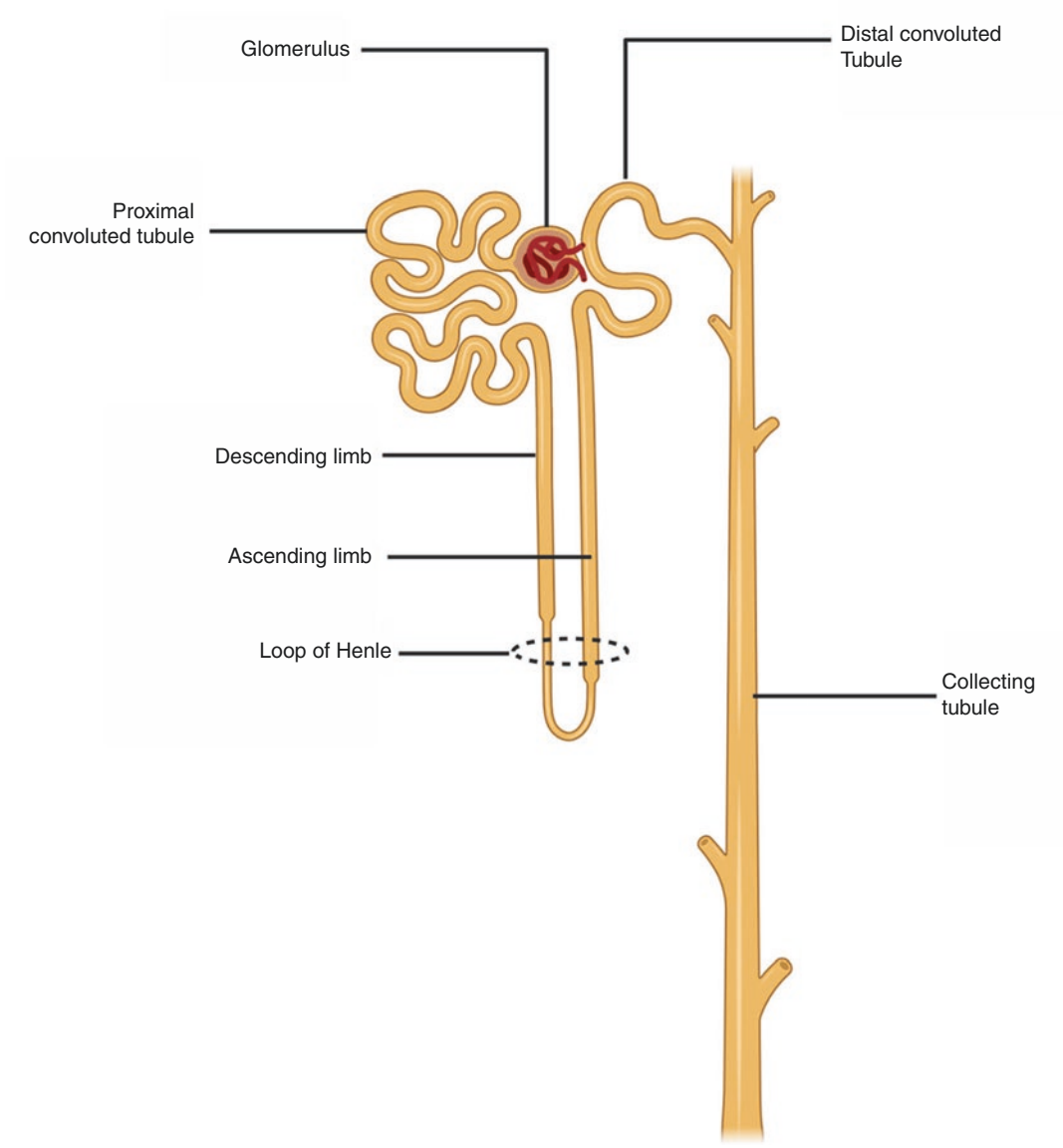

Fig. 7.2 The components of the nephron. (Created with BioRender.com)

7.1.3 Renal Vasculature

Each kidney is supplied normally by a single renal artery in the human body. However, one or more accessory renal arteries is not uncommon, which may occur in 30% of the population [3]. The renal artery enters through the hilum of the kidney and branches successively into the interlobar arteries, arcuate arteries, interlobular arteries, and afferent arterioles. Each afferent arteriole eventually branches into the glomerular capillaries. The distal glomerular capillaries merge to form the efferent arteriole. Efferent arterioles subdivide to form peritubular capillaries in the cortex or the vasa recta in the medulla. Changes in the afferent or efferent arteriolar tone play an important role in regulating the GFR.

7.1.4 Juxtaglomerular Apparatus

The afferent arteriole has specialized smooth muscle cells called juxtaglomerular (JG) cells that store renin and stretch receptors that respond to arteriolar pressure changes. Renin is released as a result of decreased stretch of the arteriolar wall when arteriolar pressure is decreased. Another stimulus for renin comes from the macula densa, which consists of specialized cells in the first part of the distal tubule, located close to the JG cells. The macula densa signals the JG cells to release renin when the sodium and chloride content of this part of the tubule is low. Finally, the sympathetic nervous system can stimulate renin release in response to systemic baroreceptor stimuli.

7.2 Renal Radiopharmaceuticals

Renal radiopharmaceuticals can be described in two broad classes—those excreted rapidly into the urine and those retained for prolonged periods in the renal parenchyma.

7.2.1 Rapidly Excreted Radiopharmaceuticals

The rapidly excreted radiopharmaceuticals are used in dynamic imaging studies to assess individual renal function and include [3–6]:

- ^{99m}Tc-mercaptoacetyltriglycine (MAG_3), the agent of choice, is 90% protein-bound and excreted almost exclusively by the renal tubules. High renal-to-background count ratios provide excellent images and permit visualization of poorly functioning kidneys.
- ^{99m}Tc-diethylenetriamine penta-acetic acid (DTPA) was the most popular radiopharmaceutical in its category prior to the introduction of ^{99m}Tc-MAG_3. It shows little protein binding (about 5%) and is excreted exclusively by glomerular filtration. Renal uptake of ^{99m}Tc-DTPA is limited because the glomeruli filter only 20% of the renal blood flow. The 20% extraction fraction is considerably lower than that of ^{99m}Tc-MAG_3 and yields lower renal-to-background uptake ratios. However, it is less costly and may be used as an alternative to ^{99m}Tc-MAG_3, particularly if a quantitative estimate of GFR is in question. Functional assessment with 99m Tc-MAG3 and 99m Tc-DTPA generally is concordant. However, differences may be noted with glomerular-tubular dissociation in some cases of tubulointerstitial disease. Orthoiodohippurate is about 70% protein bound. Approximately 15–20% of the radiotracer is excreted by glomerular filtration and the remainder by tubular secretion. The use of 131 I-OIH for scintigraphy has been largely abandoned because of the limitations of higher radiation exposure [7] and poor image quality related to a lower administered dose (1/15 that of 99m Tc-MAG3). Radiation exposure with 123 I-labeled OIH is lower, and better images can be obtained using larger amounts of the radiotracer. However, this radiopharmaceutical is expensive and not readily available. The extraction fraction of OIH, while not optimum (since it is not completely extracted by the kidneys), is the highest among the radiopharmaceuticals in use today. Therefore, it can be used for the quantification of renal blood flow.

7.2.2 Slowly Excreted Radiopharmaceuticals

The slowly excreted radiopharmaceuticals include ^{99m}Tc-dimercaptosuccinic acid (DMSA) and ^{99m}Tc-glucoheptonate. Prolonged cortical retention of these radiopharmaceuticals allows the assessment of parenchymal morphology. Since accumulation occurs only in functioning tubules, uptake can be quantified to accurately assess the differential renal function [3, 4]. The preferred agent, Technetium-99m-DMSA, is 90% protein-bound and accumulates in functioning tubules. Since very little of the radiotracer is excreted, interference from collecting system activity, particularly on delayed images, is minimal. A total of about 40% of the administered amount is accumulated in the renal cortex.

7.3 Renal Scintigraphy

According to the types of renal radiopharmaceuticals, renal scintigraphy can be of dynamic or static nature.

- *Dynamic studies* are obtained using rapidly excreted radiopharmaceuticals, while static studies are obtained utilizing slowly excreted tracers. Dynamic studies start by rapidly acquiring image frames upon injection of the tracer to follow activity passing through the blood vessels until reaching the kidneys to evaluate the blood flow. This phase is followed by another series of imaging frames every 10–20 s of the kidneys for approximately 30 min to evaluate the renal functional handling of the radiotracer. This phase will then be computer-processed to generate a time-activity curve (renogram) for both kidneys to illustrate the uptake, build up, and excretion of the radiopharmaceutical by each kidney and generate the percent contribution of each kidney to the total renal function (split or differential renal function).
- *Static studies* using slowly secreted radiopharmaceuticals, particularly ^{99m}Tc-DMSA, are acquired 3 h after intravenous injection of the radiotracer and optionally up to 24 h based on the individual case and the kidney function. These studies are predominantly used to determine the split renal function accurately and in cases of urinary tract infections to evaluate the pathologic changes, including cortical scars. Anterior, posterior, left and right posterior oblique planar views are obtained routinely with optional SPECT or SPECT/CT. Using the anterior and posterior views, the split renal function is calculated by the geometric mean of the background-subtracted kidney counts.

7.3.1 Principles of Interpretation

7.3.1.1 Dynamic Studies

Assessment of function on dynamic studies is based on several criteria, including initial cortical uptake of the radiotracer, cortical retention, first visualization of the collecting system, and time to peak cortical activity. These parameters, however, may be affected by the state of hydration. Prolonged radiotracer uptake, reduced excretion, and cortical retention can be noted in cases of dehydration [8, 9]. An adequate assessment of renal function should include analysis of both the scintigraphic images and the time-activity curves.

Cortical uptake: The first minute after radiotracer administration represents the vascular delivery phase. The next 2 min constitute the parenchymal phase. Uptake in the kidney during this interval (between 1 and 3 min after radiotracer injection) is proportional to its function, using either tubular or glomerular agents.

Cortical retention: The cortical retention of the radiotracer, quantified by expressing renal counts at 20–30 min on the time-activity curve as a percentage of the peak uptake, is a measure of the rapidity with which the kidney excretes the radiotracer. As renal function deteriorates, the percentage of retained radiotracer increases. This index can help monitor patients with renal transplants or assess renovascular hypertension [10]. An apparent increase in retention may occur with urine stasis in the collecting system.

First visualization of collecting system: The interval between radiotracer administration and excretion of activity into the collecting system (pelvis and/or calyces) is a measure of *cortical* function. This interval is obtained from the sequential images. The delayed appearance of the collecting system is associated with impaired function.

Time to peak: This parameter is easily measured from the time-activity curve. However, an accurate estimate may not be possible in the absence of a peak, which is often the case in significant renal dysfunction. Prolonged values for the time to peak can be seen in physiologic retention of the tracer in the renal calyces or pelvis [11].

7.3.1.2 Static Studies

Scintigraphy with ^{99m}Tc-DMSA and ^{99m}Tc-glucoheptonate is done between 3 and 24 h after

radiotracer administration. It is usually used to detect renal parenchymal defects associated with pyelonephritis, scars, and infarcts. Since only functioning tubular cells accumulate these radiopharmaceuticals, the total renal uptake is a measure of individual renal function. Relative renal function can also be measured as with the rapidly excreted radiopharmaceuticals.

7.4 Major Diseases

7.4.1 Renovascular Hypertension (RVH)

Approximately 5% of hypertension is renovascular in origin. It accounts for about 5.4% as a cause of secondary hypertension in adults [12–14]. Renal artery stenosis is generally due to atherosclerotic plaques or fibromuscular dysplasia, the latter occurring in younger individuals. Significant' stenosis that would trigger the activation of the renin-angiotensin system and lead to the development of renovascular hypertension has been defined as a reduction in intraluminal diameter by 50% or greater. However, the degree of anatomically defined renal artery stenosis does not always correlate with the presence of renovascular hypertension.

7.4.1.1 Pathophysiology

The renin-angiotensin system serves as maintenance of systemic blood pressure in such conditions as hypotension and shock. However, with significant renal artery stenosis, the renin-angiotensin system limits a fall in GFR but causing systemic (renovascular) hypertension. Systemic blood pressure is maintained primarily by the increase in vascular tone and sodium and water retention. At the same time, a sharp reduction in GFR is prevented by the increase in the glomerular capillary hydrostatic pressure.

Glomerular capillary hydrostatic pressure is modulated by the tone of the afferent and efferent glomerular arterioles. Increased tone in the efferent arteriole or decreased tone (increased flow) in the afferent arteriole raises capillary hydrostatic pressure and GFR. In contrast, the decreased tone in the efferent arteriole or increased tone (decreased flow) in the afferent arteriole lowers GFR.

The first step in the activation of the renin-angiotensin system is the release of *renin* by the renal JG cells by several mechanisms through [15, 16].

(1) signals from *baroreceptors* ("stretch" receptors) in the afferent arteriole modulated by prostaglandins, (2) chemoreceptor signals from the *macula densa* (located in the initial portion of the distal tubule) related to decreased sodium and chloride in the distal tubule and modulated by prostaglandins and adenosine, and (3) increased *sympathetic activity* due to activation of systemic cardiopulmonary and carotid sinus baroreceptors by hypotension.

Renin released due to these stimuli converts circulating *angiotensinogen*, an $alpha_2$ globulin produced by the liver, to *angiotensin I*, a decapeptide. Angiotensin I is then converted to the active octapeptide form, *angiotensin II*, by *angiotensin-converting enzyme* (ACE), found in vascular endothelium. The bulk of this conversion occurs in the pulmonary vascular bed. Angiotensin II is also produced in the kidney. Angiotensin II is a powerful vasoconstrictor that raises systemic blood pressure primarily by increasing vascular tone and stimulating the synthesis and secretion of aldosterone from the zona glomerulosa of the adrenal cortex, which promotes sodium and water reabsorption from the renal tubules.

The intrarenal effects of angiotensin II help counter a fall in GFR due to decreased afferent arteriolar and glomerular capillary hydrostatic pressure [15–18]. First, angiotensin II raises GFR by preferential constriction of the efferent glomerular arteriole. Second, angiotensin II increases tubular reabsorption of sodium and water directly and indirectly (increased tone in efferent arteriole decreases hydrostatic pressure in peritubular capillaries with a resultant increase in sodium and water reabsorption). GFR remains unchanged in the contralateral normal kidney in unilateral renal artery stenosis

because the increased efferent arteriolar tone is offset by an increase in afferent arteriolar tone in response to a higher systemic blood pressure. The effects of angiotensin II eventually lead to inhibition of renin release. In unilateral renovascular disease, sodium retention is offset by pressure natriuresis (decreased sodium chloride reabsorption in the proximal tubule) by the normal kidney. The process limits the expansion in blood volume, so the pressure in the afferent arteriole of the stenotic kidney remains low. In bilateral renovascular disease, however, blood volume expansion may be sufficient to increase afferent arteriolar pressure and decrease (but not necessarily normalize) renin secretion. Angiotensin II also has a direct inhibitory effect on the JG cells.

7.4.1.2 Scintigraphy for RVH

Basis

The scintirenographic diagnosis of renovascular hypertension is based on the demonstration of renal physiology changes following the administration of an ACE inhibitor [19–21]. As noted above, angiotensin II, formed by the activation of the renin-angiotensin system, helps maintain GFR by increasing the tone of the efferent glomerular arteriole, raising the glomerular capillary hydrostatic pressure. These changes are reversed by ACE inhibitors, which block the conversion of angiotensin I to angiotensin II. Consequently, there is a sharp drop in GFR and proximal tubular urine flow.

Decreased GFR and tubular flow after administering an ACE inhibitor will decrease uptake and prolonged cortical retention of ^{99m}Tc-DTPA. Since renal blood flow generally is not significantly changed, ^{99m}Tc-MAG_3 shows only prolonged cortical retention without decreased uptake. Rarely, uptake of ^{99m}Tc-MAG_3 may decrease, presumably due to a fall in blood pressure below a critical level required to maintain perfusion in the stenotic kidney. The general principles of ACE-inhibitor renography also apply to patients receiving chronic treatment with angiotensin II (AT1) receptor antagonists [22].

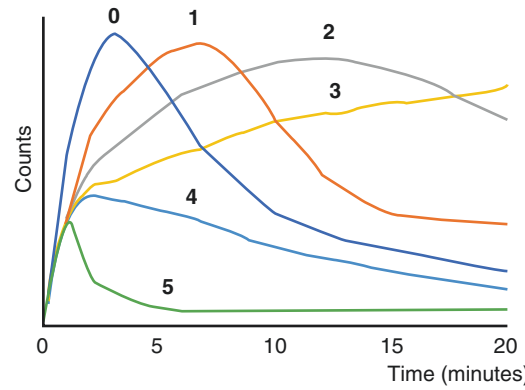

Fig. 7.3 Renographic curve patterns with the grading of suspicion for renovascular hypertension: 0, normal; 1, minor abnormalities; 2, delayed excretion rate with preserved washout phase; 3, delayed excretion rate without washout phase; 4, renal failure pattern with measurable kidney uptake; 5, renal failure pattern without measurable kidney uptake (blood-background type curve). (Adapted from [24])

Interpretation

Scintigraphic studies are generally interpreted by comparing a baseline examination with the one performed after the ACE inhibitor administration. Visual analysis of the time-activity curves of both kidneys using a grading system as shown in Fig. 7.3 can be a valuable method to define the degree of suspicion of renal artery stenosis [23]. Both the images and the time-activity curves are evaluated using the traditional parameters of function discussed earlier, and the following changes after ACE inhibition are considered significant for renovascular hypertension [21–24]:

1. Increase in cortical retention by at least 15% or a change ≥2 in the renogram grade, i.e., 0 to 2 or 1 to 3.
2. Delay in collecting system visualization by at least 2 min.
3. Decrease in initial cortical uptake by at least 10%.
4. Increase in time to peak by at least 2 min.

Factors Influencing ACE Inhibitor Scintigraphy

ACE inhibitor renography is subject to several variables that may result in false-positive or false-negative studies.

1. Hypotension or a marked change in blood pressure after ACE inhibitor administration is often associated with *bilateral symmetrical* renal retention of the radiotracer.
2. Dehydration with or without diuretics. An additional oral fluid load of 5–10 mL/kg of body weight 30–60 min before the procedure is advised to ensure proper hydration [25, 26].
3. Chronic ACE inhibitor therapy may potentially lower scintigraphic sensitivity and should be discontinued before the test. Alternatively, if the ACE inhibitor cannot be discontinued, scintigraphy may be performed while the patient is on therapy. If renal function appears symmetrical, renovascular hypertension is unlikely, and a baseline study need not be done. However, if the function is asymmetrical, the ACE inhibitor should be discontinued before the baseline study.
4. Aspirin and other nonsteroid anti-inflammatory agents such as indomethacin may decrease the sensitivity of the test. These drugs decrease prostaglandin activity and, therefore, indirectly decrease renin-angiotensin activity. This is particularly true with the use of DTPA, and hence MAG_3 is preferred in patients who take nonsteroidal anti-inflammatory drugs [24].
5. Calcium channel blocking drugs are commonly used in renovascular hypertension. Although their effect on GFR is not as pronounced as that of ACE inhibitors, these drugs have been implicated as a cause of false-positive studies [27]. The mechanisms responsible for this finding are not entirely clear. It appears that the effect of angiotensin II on efferent arteriolar constriction requires the presence of extracellular calcium and, therefore, can be attenuated by calcium channel blockers. Perhaps a marked decrease in GFR resulting from the combined effect of calcium channel blockers and captopril may explain the above findings.

7.4.2 Urine Outflow Obstruction

Urinary tract obstruction may be complete or partial, and it may occur at various locations, including the ureteropelvic junction (UPJ), ureterovesical junction (UVJ), and bladder outlet. The clinical consequences are quite dramatic and predictable in an acute and complete obstruction, but not in a partial and chronic one, exemplified by UPJ obstruction in children. Chronic UPJ obstruction, however, may eventually lead to renal cortical atrophy.

Hydronephrosis may be due to obstruction or non-obstructive conditions such as vesicoureteral reflux, urinary tract infection, and congenital dysmorphism. It may be temporary with spontaneous resolution in infants and young children, intermittent, or progressive with eventual stabilization.

7.4.2.1 Diuretic Renography

Furosemide, used for the scintigraphic evaluation of urine outflow for diagnosis of urinary tract obstruction, and other loop diuretics block the reabsorption of sodium, chloride, and potassium in the thick ascending limb of the loop of Henle. Increased tubular sodium decreases water reabsorption by an osmotic effect. Additionally, decreased sodium reabsorption into the medullary interstitium reduces its osmolarity, which in turn reduces water reabsorption from the collecting tubules.

Diuretic renography [28–31] is based on the principle that increased urine flow resulting after furosemide administration causes rapid "washout" of radiotracer from the unobstructed collecting system (Fig. 7.4), but delayed washout is noted if obstruction is present (Fig. 7.5). While furosemide generally is administered intravenously after filling the pelvicalyceal system, administration at the time of or before radiotracer administration has also been used. The standard adult dose of furosemide is 0.5 mg/kg or 40 mg, producing maximal diuresis within 3–6 min in patients with normal renal function. A higher dose of furosemide may be required in patients with impaired renal function to achieve an adequate diuretic response [32]. The washout half-time following diuretic injection is determined from the time-activity curve. A half time of 10 min or less is considered normal, 10–20 min equivocal, and more than 20 min abnormal. However, over-reliance on the washout half-time may not be justified because many factors may

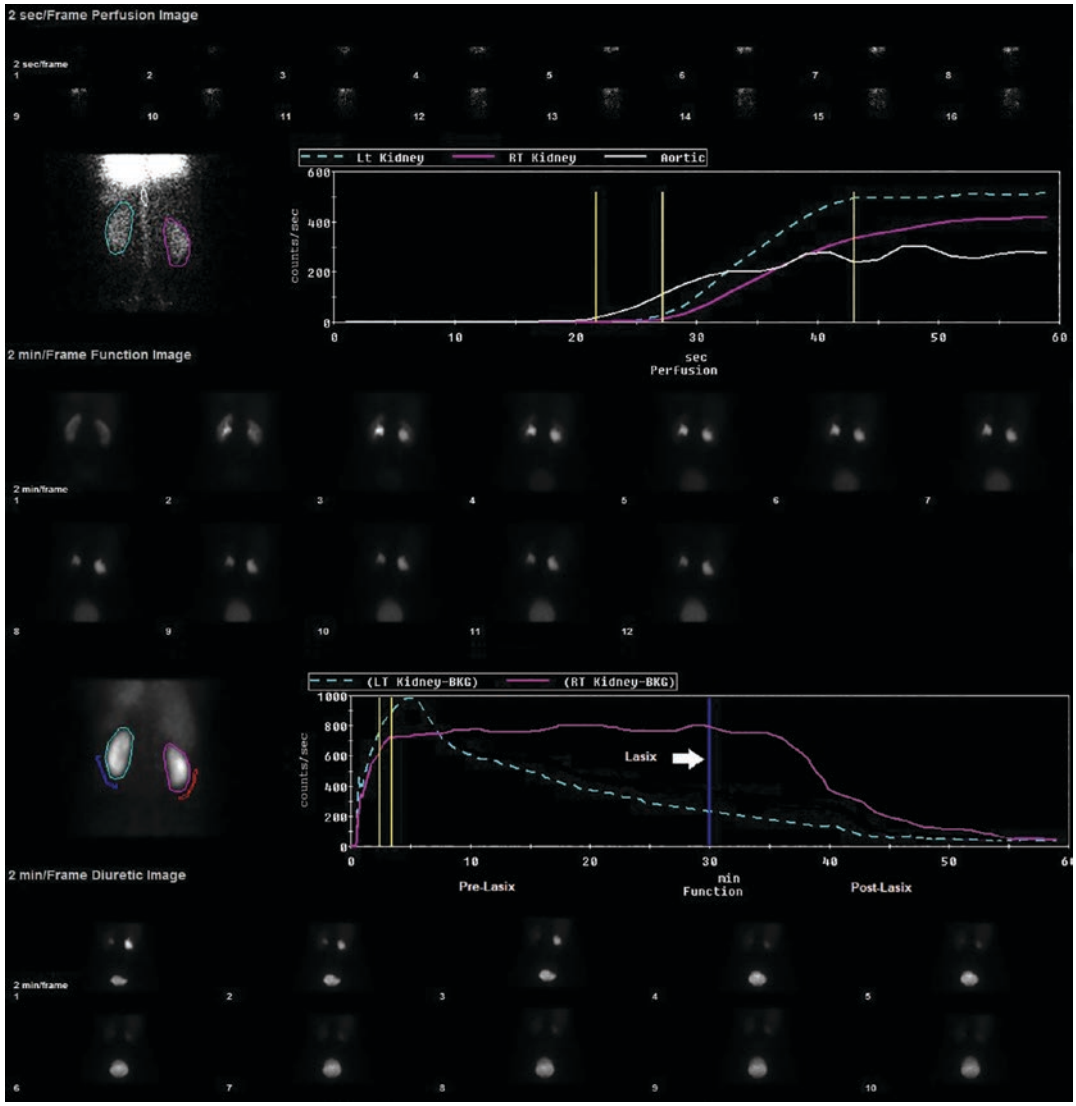

Fig. 7.4 A radionuclide diuretic renography study is illustrating hold-up activity in the right functioning kidney by the end of the pre-Lasix study with rapid washout on post Lasix study, which is clearly illustrated on the time-activity curve. These exemplify the non-obstructed pattern

influence the diuretic renogram, including renal dysfunction, dehydration, inadequate furosemide dosage, atonic pelvis (redundant tissue).

Some steps may be taken to optimize the radionuclide evaluation of urinary tract obstruction. Since renal function preservation is the overriding concern, it has been suggested that renal cortical function evaluation should be the primary focus of scintigraphic assessment. Additionally, since renal impairment or its progression is unpredictable, a single study in the infant with UPJ obstruction is of limited value. Instead, *periodic scintigraphic assessments* at intervals of 3 months are more desirable. Undue reliance on a single post-diuresis washout half-time also appears unwarranted for the reasons noted earlier. If the methodology is standardized, periodic evaluation as for functional assessment may improve the predictive ability of the washout parameter as well. An increasing washout time probably is more meaningful than a single "positive" study [28].

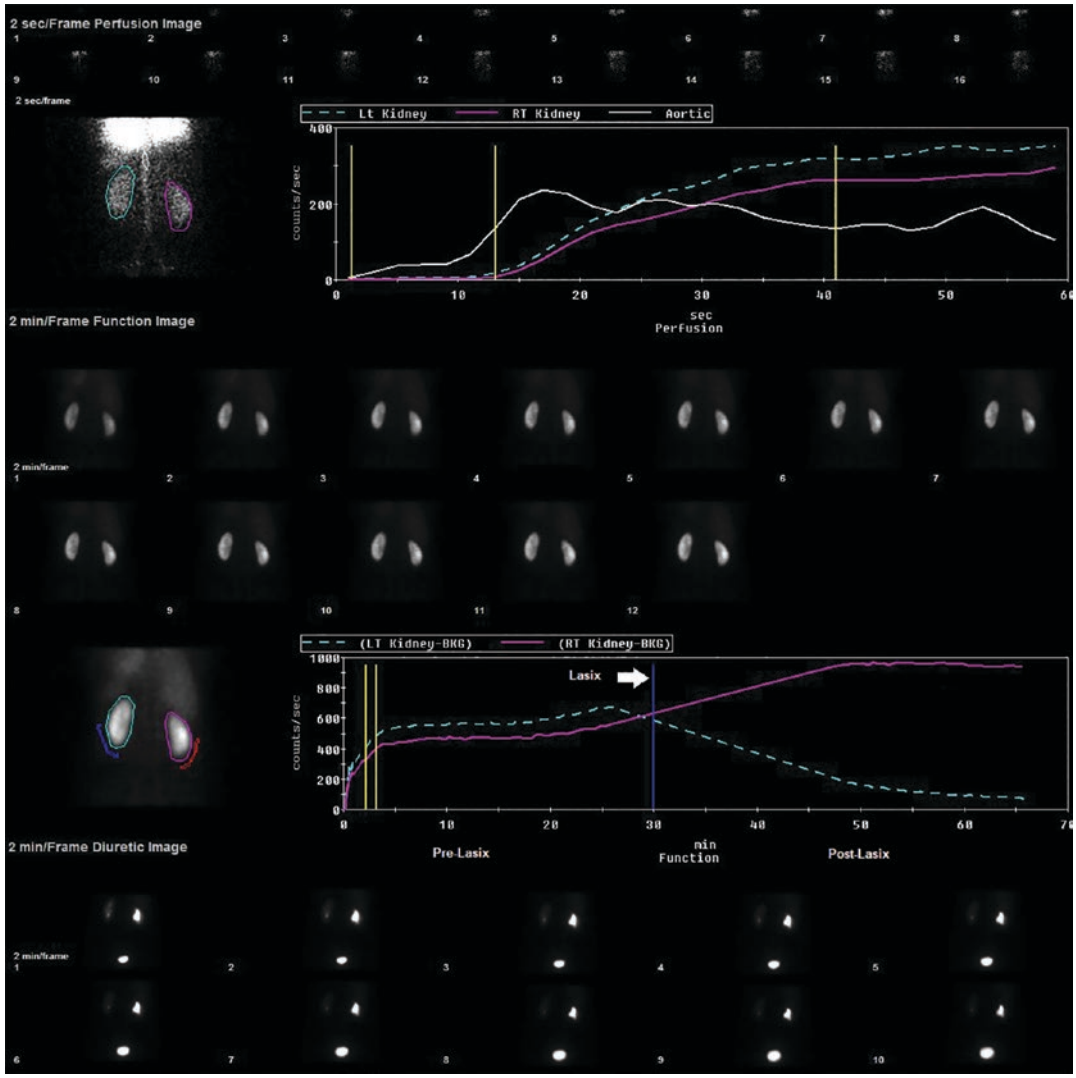

Fig. 7.5 A diuretic renography study in an adult patient illustrating obstructive pattern on the left side. Note the left kidney time activity curve, which shows no clearance before Lasix and no response to Lasix

7.4.3 Urinary Tract Infection

7.4.3.1 Pathophysiology

Urinary tract infections (UTIs) are particularly important in the pediatric age group as it is one of the most common diseases in children. UTIs' overall incidence in children ranges between 1.5% and 2% [29–31]. In the neonatal period, UTIs are relatively rare and are usually caused by bacteria from the bloodstream. The incidence in newborns is higher for boys, while girls are affected (1%) more than boys (0.3%) between the ages of 1 and 5 years [29–31]. The incidence increases up to 5% among girls of school age. The most common age for UTIs in girls is 7–11 years, resulting from bacterial infection – usually a pathogenic strain of *Escherichia coli*—ascending the urethra.

Many predisposing factors affect the incidence and the severity of the disease in different age groups. These factors include individual susceptibility, bacterial virulence, and the host's anatomical abnormalities such as the presence of vesicoureteral reflux (VUR), obstruction, stasis,

Table 7.1 Factors predisposing to and affecting the severity of UTI in children

Individual susceptibility
Bacterial virulence
High-grade vesicoureteral reflux
Obstruction and stasis
Hydronephrosis with or without pelviureteric junction obstruction
Horseshoe kidney
Crossed renal ectopia
Renal duplication with ectopic ureters
Urethral polyps or diverticula
Posterior urethral valves or ureterocele
Lack of circumcision (boys)
Sexual activity (girls)
Indwelling urinary catheter
Trauma to the urinary tract
Diabetes

or stones (Table 7.1). However, UTIs may also occur in healthy children with an anatomically normal urinary tract. Individual susceptibility may be variable and can be related to familial or hereditary factors.

Chronic pyelonephritis is a result of recurrent or untreated acute pyelonephritis. It occurs almost exclusively in patients with major anatomic anomalies, including urinary tract obstruction, renal dysplasia, or, most commonly, vesicoureteral reflux (VUR) in young children.

Although pseudomonas infection is common in UTIs following reflux, particularly the severe cases [33], the usual pathogenesis of UTIs is the proliferation of *E. coli* in the colon. This bacterial proliferation allows the movement of the bacteria into the periurethral mucosa. To be able to multiply, bacteria that reach the urinary tract must overcome the tendency to be washed away by urine flow and bladder voiding. Accordingly, prolonged intervals between voiding, increased storage pressure, or significant residual urine volume favor bacteria's growth and allowed even relatively nonpathogenic bacteria to cause significant infections. Vaginal filling secondary to high voiding velocity and turbulent urine flow related to a dysfunctional voiding pattern is an important factor in bacterial contamination and urinary infections in girls [34].

Urinary tract infections are divided into lower and upper infections. Lower UTI or infection of the bladder (cystitis) results in mucosal inflammation and congestion, which causes hyperactivity of the detrusor muscle and decreasing the bladder capacity [35]. This also can lead to urine reflux up the ureter. This reflux can send bacteria to the kidney, leading to acute or chronic pyelonephritis, which may cause renal abscesses or scarring. Acute pyelonephritis requires more vigorous treatment than lower urinary tract infection and, if left untreated, can lead to scarring and renal insufficiency. Consequently, identifying renal involvement is critical in children with suspected urinary tract infection and parenchymal scintigraphy with the tubular agent, Tc-99m-dimercaptosuccinic acid (DMSA), can play an important role in their diagnostic evaluation.

Ascending infection from the lower urinary tract is the usual cause of pyelonephritis. The infection appears to originate in the urethra or the vaginal introitus, colonized by enteric flora, predominantly *Escherichia coli*. It is more common in females, presumably due to their shorter urethra. The ascending infection eventually reaches the renal calyces, from which micro-organisms enter the parenchyma through the papillae by intrarenal reflux.

Severe long-term sequelae, such as hypertension and renal failure, may develop if urinary infection leads to acute pyelonephritis and subsequently to renal scarring. The pathophysiology of renal scarring is still obscure. Numerous factors may contribute to tissue damage following acute infection. It was found that patients with increased Transforming growth factor-beta1 (TGF-beta1), a potent proinflammatory and fibrogenic cytokine known to have a key role in regulating the renal tissue fibrosis, may be at higher risk for renal damage following reflux [36].

Nonsecretor status of blood type antigen has also been associated with a higher risk of urinary tract infection (UTI) in women. A study has shown that the nonsecretor status significantly correlated with the presence of focal renal scarring (41% vs. 22% for children with and without scarring, respectively) as determined by ^{99m}Tc-DMSA renal scan [37].

Scarring of the renal parenchyma is a common cause of hypertension and, if sufficiently extensive, can lead to progressive renal insufficiency and end-stage renal disease. Vesicoureteral reflux, particularly of a higher grade, is frequently associated with scarring.

The upper UTIs cannot be easily differentiated clinically from cystitis based only on symptoms. However, differentiation between upper and lower UTI is important since the former is often associated with renal parenchymal damage. It is particularly difficult in infants, who usually develop nausea, vomiting, diarrhea, or jaundice. In children, fever, frequency, urgency, enuresis or incontinence in a previously dry child, abdominal pain, foul-smelling urine, and sometimes hematuria are the most common clinical presentations. It is estimated that up to 40% of children with UTI are asymptomatic [38].

7.4.3.2 UTI Scintigraphy

Imaging strategies in pediatric urinary tract infections are controversial. The recent literature illustrates the complementary roles of ultrasound, computed tomography (CT), and nuclear medicine [39–41].

Imaging renal parenchyma with ^{99m}Tc-DMSA offers a simple and accurate method for detecting acute pyelonephritis in a child with urinary tract infection. ^{99m}Tc-DMSA localizes in functioning proximal tubular cells and is not excreted in significant amounts. Imaging at 3–24 h after radiopharmaceutical administration reveals primarily cortical uptake without interfering activity in the collecting system. A cortical defect due to pyelonephritis is characterized by the preservation of renal contour, whereas scarring (from a previous infection) typically results in organ volume contraction (Fig. 7.6).

In addition to imaging during the acute phase of the disease, follow-up studies are done to confirm the resolution of the pyelonephritic defect(s) and the absence of cortical scarring. Patients with scars are followed periodically with imaging and relative function measurements to assess for progressive renal insufficiency (Fig. 7.7).

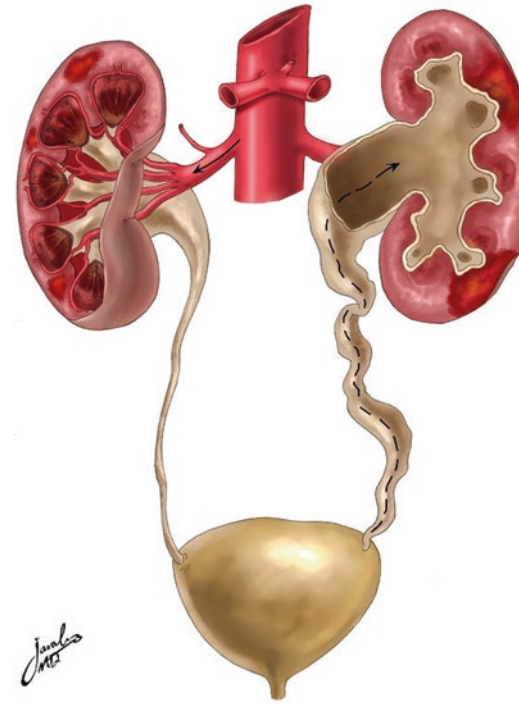

Fig. 7.6 Diagram illustrating the routes of inducing urinary tract infection. The *left-hand side* represents the hematogenous route, while the *right-hand side* represents the retrograde route such as with vesicoureteral reflux

The importance of ^{99m}Tc-DMSA for patients with urinary tract infections for initial evaluation and follow-up of children with UTI was re-emphasized by many studies [42–45].

Ultrasonography is recommended by newer guidelines to be used more than before; Spiral CT and Magnetic resonance imaging (MRI) are other modalities that may help evaluate pyelonephritis [40, 41].

7.4.4 Renal Transplantation Complications

Renal transplantation surgery has shown significant improvement in graft survival and an increase in the number of transplantations. Graft survival is best when the donor is an HLA-identical sibling and better for living-related than cadaver donors with similar HLA matches. Other factors, including harvesting and transplantation technique, cold

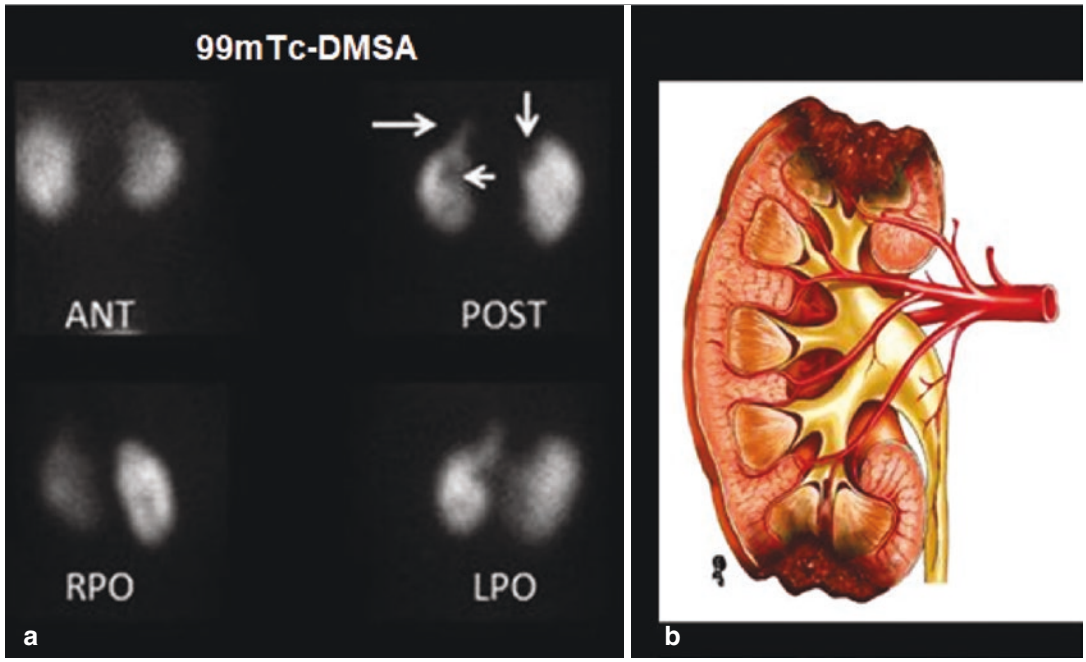

Fig. 7.7 ^{99m}Tc-DMSA study (**a**) demonstrating bilateral upper pole defects and a mid-left kidney defect (arrows). A diagram (**b**) illustrates how scars affect the kidney contour

ischemia time (between harvest and transplantation), donor/recipient age, recurrence of primary renal disease, and race, also play an important role in graft survival. Several complications, surgical and/or medical (Table 7.2), occur following transplantation and need to be detected and evaluated to avoid graft failure and outcome.

Table 7.2 Renal transplantation complications

Surgical complications
Urine extravasation, ureteral obstruction
Hematoma, lymphocele
Renal artery stenosis
Medical complications
Acute tubular necrosis
Rejection
Antibody-mediated rejection
Hyperacute rejection
Accelerated acute rejection
Acute/active rejection
Chronic/sclerosing allograft nephropathy
Nephrotoxicity of drugs

7.4.4.1 Surgical Complications

Urine Extravasation, Ureteral Obstruction

Extravasation of urine ("urinoma") may result from ischemic injury related to devascularization during harvesting or leakage at the ureterovesical anastomosis. It may predispose to infection and therefore requires a timely diagnosis. While routine renal scintigraphy performed after transplantation may detect urine extravasation, it is often used to confirm a leak suspected clinically or sonographically. The scintigraphic appearance is an area of increased radiotracer activity, although such increase may not be apparent for up to 2–3 h after radiotracer administration in some instances.

Ureteral obstruction is thought to be usually due to ischemia or postischemic scarring. Extrinsic compression by a lymphocele or hematoma is another cause. If needed, dilatation of the ureter or stent placement/reoperation may be done. Scintigraphy, with the aid of furosemide-induced diuresis in some cases, maybe helpful in the diagnosis and post-treatment evaluation of this condition.

Hematoma, Lymphocele

Hematomas are generally perinephric or intravesical in location. Scintigraphy can be positive, demonstrating a photopenic region, i.e., with activity less than the background. Hematomas are usually self-limited.

Lymphoceles are extrarenal collections of lymphatic fluid from the kidney, occurring most frequently about 2–3 months after transplantation. They may be exacerbated by rejection, which increases renal lymph flow. Most lymphoceles are inconsequential, though some may be associated with ureteral compression, as noted earlier, or iliac vein compression resulting in lower extremity edema. Treatment consists of sclerotherapy, drainage, or the creation of a peritoneal window. The characteristic scintigraphic finding with lymphoceles is a perinephric photopenic region, which is easier to visualize if a high-intensity image is obtained at the end of the study to accentuate the body background. However, it should be noted that lymphoceles occasionally may become isointense with the background or exceed background activity on later images.

Renal Artery Stenosis

Hypertension is usually due to pathology in the native kidneys, transplant rejection, or cyclosporine/tacrolimus treatment, and, less frequently, renal artery stenosis. The stricture is generally at the anastomotic site or distal to it. The pathophysiological consequences of renal artery stenosis in the transplanted kidney are somewhat different from unilateral stenosis in patients with two kidneys. In the latter, the elimination of sodium is decreased on the stenosed side, but increased sodium excretion by the normal kidney helps keep the blood volume from increasing. In a transplanted kidney with renal artery stenosis, a normal kidney is not available to eliminate excess sodium. Therefore, depending on the level of salt intake, the initial renin-dependent hypertension develops into volume-dependent hypertension. Consequently, the fall in GFR in response to an ACE inhibitor may be less than expected and inapparent on the scintigraphic study. However, most of these patients are on diuretics and/or a salt-restricted diet, which will help to limit the rise in blood volume.

7.4.4.2 Medical Complications

Acute Tubular Necrosis

Acute tubular necrosis (ATN), characterized by ischemic necrosis of the tubular epithelial cells and decreased GFR, is frequently associated with cadaver renal transplants. Possible causes are hypotension/hypovolemia in the donor and the prolonged interval between harvest and transplantation. Urine output usually starts to decrease within the first 24 h or so and improves spontaneously after a few days, although ATN may occasionally last a few weeks. It is often difficult to make a clinical distinction between ATN and rejection in the post-transplantation period. A clear scintigraphic distinction between these two conditions also has remained elusive for two reasons. First, the scintigraphic diagnosis of ATN rests on the premise that graft perfusion is preserved despite decreasing function (Fig. 7.8), in contrast to rejection, where both perfusion and function decrease in parallel (Fig. 7.9). However, depending on the severity/stage of ATN, graft perfusion may vary. Second, ATN and acute rejection may coexist. From a clinical standpoint, a cadaver transplant with impaired function is assumed to have ATN. An aggressive search/treatment for rejection is initiated if the expected recovery in graft function fails to occur. Such recovery can best be ascertained by serial scintigraphy, a sensitive measure of graft function, although the two may be indistinguishable.

Rejection

The histopathological criteria for the diagnosis and classification of rejection have improved significantly in recent years and continue to evolve [46–48]. From a large body of literature, a consensus referred to as the *Banff Classification* has emerged. The new classification shifts the focus from diagnosis of rejection to prognosis to facilitate patient management. The distinction is made between rejection with *tubulointerstitial* changes, milder disease, and rejection with *vasculitis*, where the outcome is poorer. The types of rejection are discussed below.

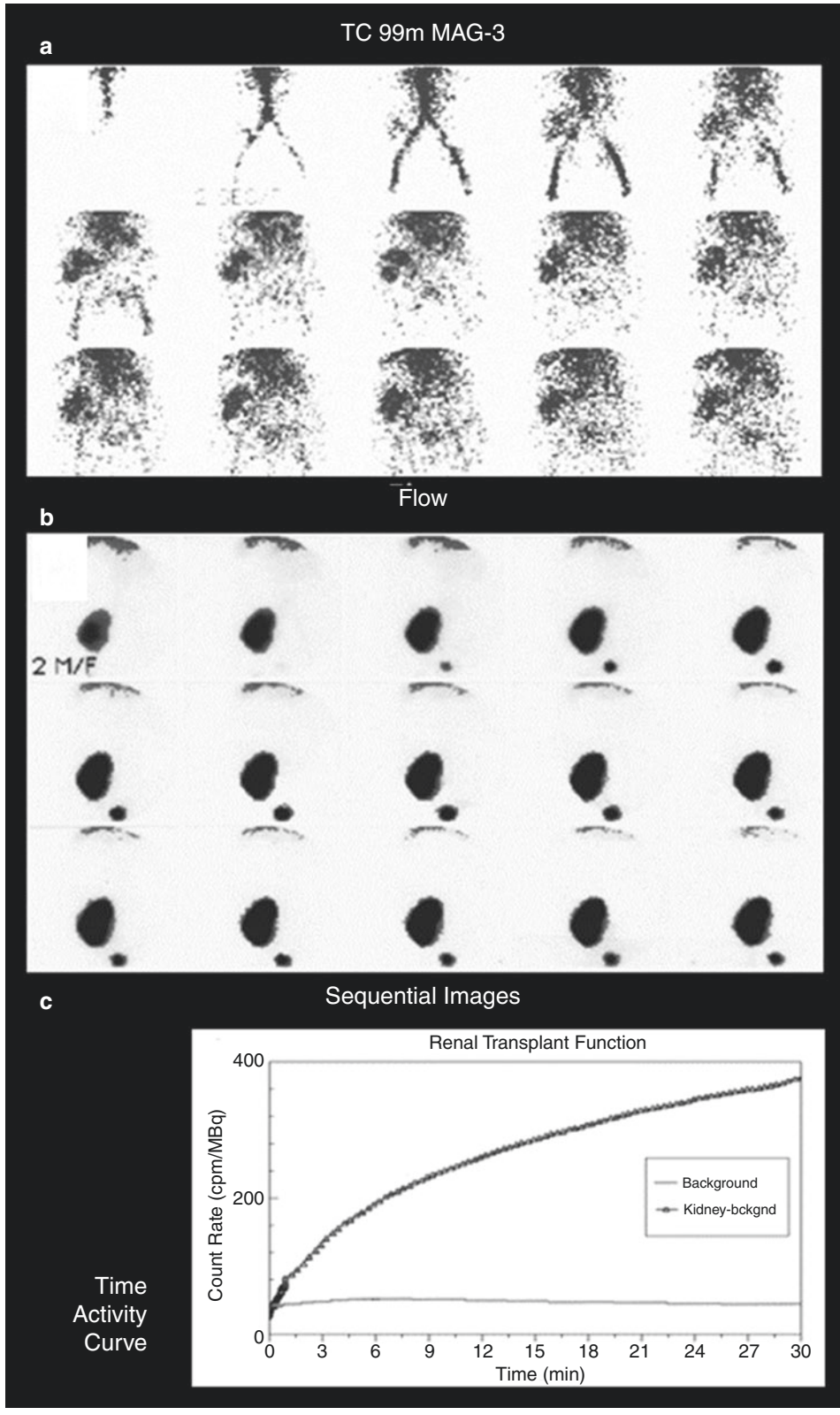

Fig. 7.8 Acute tubular necrosis following renal transplantation. The perfusion is preserved (**a**), while the renal dysfunction is noted through the parenchymal retention (**b**) and rising time-activity curve (**c**). (Courtesy of Dr. A. Omar)

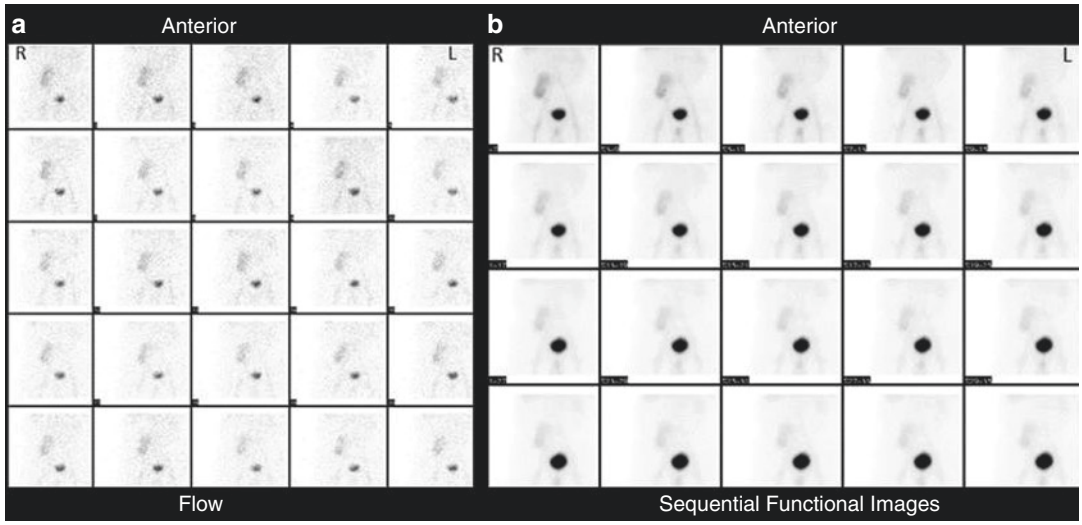

Fig. 7.9 Tc 99m MAG-3 study for a patient with renal transplantation showing decreased perfusion (**a**) and function (**b**) of the graft illustrating the scintigraphic findings of rejection

1. Antibody-mediated rejection:

   Two types of antibody-mediated rejection are described, immediate or hyperacute and delayed or accelerated acute. *Hyperacute rejection* is caused by preformed anti-donor antibodies and is characterized by intense vasculitis, fibrin-platelet thrombi, and infarction of the renal cortex, with graft loss. Rejection may begin within minutes or hours and is usually apparent during surgery. Scintigraphy shows a *photopenic* region corresponding to the avascular graft. Fortunately, hyperacute rejection is rare nowadays and largely preventable by appropriate screening tests.

   Accelerated acute rejection may be considered a "slow" variant of hyperacute rejection, mediated primarily by anti-donor antibodies. It usually occurs on the second or third day following transplantation, after allograft function has been established. Clinical manifestations include fever, pain, swelling, tenderness in the transplant region, hypertension, oliguria, or anuria. Scintigraphy generally shows poor radiotracer uptake in the graft.
2. Acute/active rejection:

   Acute rejection is the most frequent type of rejection confronting the nuclear medicine physician. It is most common in the first 4 weeks following transplantation but may occur at any time between 3 days and 10 or more years. Clinical findings generally are not as dramatic as in accelerated rejection. Acute rejection is predominantly a cell-mediated process with mononuclear cell infiltration and tubulitis, although the more severe forms are associated with a humoral component with various degrees of vasculitis. Accordingly, the Banff system grades acute rejection from I to III, with subdivisions for the severity of changes. The lowest grade represents interstitial infiltration and moderate tubulitis, while the highest grade is associated with transmural arteritis and/or arterial fibrinoid change and necrosis of medial smooth muscle cells.
3. Chronic/sclerosing allograft nephropathy:

   Generally occurs 6 months to years after transplantation. It may be related to many causes, including chronic rejection, hypertension, infectious/noninfectious inflammatory process, and medications' effects (see below). If present, rejection may respond to treatment, though the diagnosis may not be apparent on biopsy. Histopathological changes in the condition also can be graded, depending on the severity of interstitial fibrosis and tubular atrophy.

Nephrotoxicity of Drugs

Cyclosporine and, more recently, tacrolimus (FK506) have been used routinely as immunosuppressive agents. Clinically, nephrotoxicity resulting from these drugs may be difficult to distinguish from rejection, and the conditions may be superimposed. Toxicity is generally associated with elevated blood levels of the drug, improving after dose reduction. Histopathological findings of microvascular injury, with fibrin thrombi in the glomerular arterioles and capillaries, have been noted but, unfortunately, are not diagnostic for cyclosporine or tacrolimus toxicity [49–51].

7.4.5 Vesicoureteral Reflux

7.4.5.1 Pathophysiology

VUR is the retrograde flow of the urine from the bladder into the ureter. Normally, urine is propelled from the kidney to the urinary bladder through the ureter in only one direction. The valvular role of the ureterovesical junction depends on the anatomical relationship between the ureter and the bladder. The ureter follows a retroperitoneal course from the kidney to the bladder. After penetrating the bladder wall, the ureter is securely anchored to it throughout its entire transmural course. A specific arrangement serves to maintain a competent one-way valve at the ureterovesical junction with a mechanism that is best described as a flap valve.

VUR allows the infected urine to be repeatedly returned to the kidneys from the bladder, and the reflux drains back into the bladder at the end of each voiding. Pyelonephritis, especially in children younger than 3 years, is often a result of combined reflux and infection. VUR occurs more frequently in girls by a ratio of 10:1, and the incidence is approximately 1 in 1000 children. Reflux may be unilateral or bilateral and is commonly classified by the international radiologic grading system (Table 7.3). The international radiologic grading includes five grades using detailed anatomy, such as the characterization of the fornices that are impossible to achieve by scintigraphic studies. Accordingly, a more simplified scintigraphic grading attempt classifies reflux into three grades (Table 7.4 and Fig. 7.10) grades; mild (I), moderate (II), and severe (III) [52].

Table 7.3 Radiologic grading of vesicoureteral reflux

I	Reflux into a non-dilated ureter.
II	Reflux into the upper collecting system without dilatation.
III	Reflux into mildly dilated ureter and pelvicalyceal system.
IV	Reflux into a grossly dilated ureter and pelvicalyceal system.
V	Massive reflux with marked ureteral dilatation and tortuosity and marked dilatation of the pelvicalyceal system.

Table 7.4 Scintigraphic grading of vesicoureteral reflux

Grade I	Reflux into the ureter.
Grade II	Reflux into the pelvicalyceal system.
Grade III	Reflux into the pelvicalyceal system with apparently dilated pelvis or both pelvises and ureters.

The flap mechanism of the ureterovesical junction depends on several anatomical relationships and physiological parameters. Any condition that alters these relationships can lead to reflux. Examples include abnormal obliquity of the ureter during its intramural course, conditions that weaken the bladder's muscular support to the ureter, and sphincter dyssynergia. VUR may be primary or secondary [53, 54].

Primary reflux results from a congenitally abnormal or ectopic insertion of the ureter into the bladder. Occasionally, the condition is hereditary [55]. Siblings of patients with vesicoureteral reflux (VUR) are at greater risk of reflux than the general population, and screening in this group is widely accepted. In a recent study, at 48 months after diagnosis, 75% of mild reflux cases (I–III) and 37% of severe reflux (IV and V) of prenatally detected primary VUR had resolved, indicating a relatively benign clinical course.

Secondary reflux is more serious and may be transient or persistent [35]. It develops in association with infection, malformations of the ureterovesical junction, increased intravesical pressure, and surgery to the ureterovesical junction.

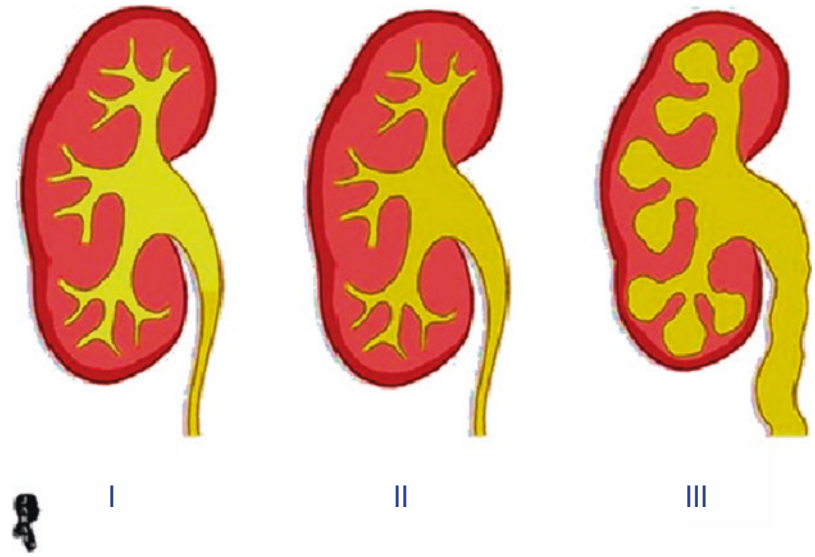

Fig. 7.10 Grades of vesicoureteral reflux used for radionuclide studies

The interstitial cells of Cajal (ICCs) are pacemaker cells that create and coordinate peristaltic motility. It was recently found that refluxing ureteral endings significantly lack these pacemaker cells, implying a malfunctioning valve mechanism permitting VUR. Connexin 43 (gap junction protein) immunoreactivity was significantly decreased in all refluxing ureteral specimens, whereas; it was homogeneously distributed in normal controls. A substantial decrease in gap junctions in this region adversely affects intercellular signaling, aggravating coordinated peristalsis, which is essential for a competent anti-reflux mechanism [53].

7.4.5.2 Reflux Scintigraphy

Voiding radionuclide cystography is a sensitive procedure for the early detection and monitoring of VUR. Early diagnosis of VUR with subsequent follow-up helps to prevent cortical scarring. It is especially attractive because of its excellent sensitivity and low absorbed radiation dose compared with the radiographic MCUG. It was estimated that its radiation exposure is less than 1/20 of the conventional contrast-enhanced micturating cystourethrogram (MCU) [53]. The sensitivity of indirect voiding urosonography without contrast media and without filling the bladder through a catheter to detect vesicoureteral reflux (VUR) in children is inadequate; its overall sensitivity is only 49% [56].

Approximately 20% of patients with vesicoureteral reflux diagnosed before 6 months of age demonstrated dysfunctional voiding after the age of toilet training [57]. Accordingly, follow-up of patients is important. The duration and methods of follow-up of VYR patients are controversial. Voiding cystography, however, may not be used in certain groups of patients for routine follow-up. For instance, the follow-up of uncomplicated ureteral reimplantation in children is usually done by ultrasonography. Additionally, in this group of patients, follow-up for more than 1 year postoperatively is not warranted, and ultrasonography can be eliminated beyond the year [57].

Similarly, ultrasonography is used for screening for siblings of patients with vesicoureteral reflux who are at higher risk than the general population. If ultrasonography is abnormal, the gold-standard test, the radionuclide voiding cystography, is performed [58].

On the other hand, follow-up of newborns with prenatally detected VUR might require voiding cystourethrogram (VCUG) and DMSA scan. In a study [59], 58% of such infants had bilateral VUR. Severe reflux (grades IV and V) was more common and present in 54% of infants. Renal damage was detected in 34% of the kidneys on the first renal scan, with a significant correlation between severe reflux and renal damage scars [59].

Generally, voiding cystourethrograms are associated with significant trauma to patients and should not be used routinely according to the recent guidelines. VCUG is indicated if renal and bladder ultrasonography reveals hydronephrosis, scarring, or other findings that would suggest either high-grade vesicoureteral reflux (VUR) or obstructive uropathy, as well as in other atypical or complex clinical circumstances [40, 41].

7.4.6 Testicular Torsion

7.4.6.1 Pathophysiology

Testicular torsion occurs when the spermatic cord is twisted, and it has been argued that the correct term should be spermatic cord torsion [60, 61]. Although various factors may predispose to torsion [62], a narrow mesenteric attachment from the spermatic cord to the testis and epididymis is regarded as the dominant cause, i.e., a slender attachment occurring as a result of a narrowed testicular bare area. This bare area may reach nearly one-third of the testicular circumference, allowing the testis to fall forward within the cavity of the tunica vaginalis and to rotate like a bell-clapper; the intravaginal type of torsion [63].

Other forms of testicular torsion are recognized. In neonates, the gubernaculum is not attached to the scrotal wall, and the testis is susceptible to torsion. This is termed extravaginal torsion, as the entire testis, epididymis, and tunica vaginalis twist in a vertical axis on the spermatic cord. Some vestigial testicular appendages are susceptible to torsion. There are four testicular appendages: the paradidymis (organ of Giraldés), the appendix testis (hydatid of Morgagni), the appendix epididymis, and the vas aberrans of Haller (divided into superior and inferior components). The appendix testis was most consistently present in 92% of autopsies and found to be multiple in 8% [63, 64].

Two factors are critical in testicular torsion: the extent of spermatic cord twist and the torsion duration. The degree of torsion can vary from 90° to three complete turns of the vascular pedicle. Not surprisingly, blood flow may be variably compromised. The initial disruption will be to the venous and lymphatic drainage, rather than to the arterial input of the testis, and venous infarction occurs earlier and at lesser levels of torsion [65].

Experimentally, complete cessation of blood flow to the testis occurs with the spermatic cord twisting 720° [66]. A 450° twist consistently produced no flow and testicular infarction in the normal rabbit testis, whereas a 360° twist resulted in decreased flow [67].

In patients with torsion, a twist between 360° and 720° is found. Experimental studies have shown that testicular infarction begins to appear within 2 h of complete occlusion of the testicular artery [67]; irreversible ischemia occurs after 6 h [68–70], and complete infarction is established by 24 h.

With complete vascular occlusion, the testis appears grossly swollen and hemorrhagic. Microscopically, the picture is that of hemorrhagic infarction. The degree of necrosis depends upon the duration of occlusion. If this has been longer than 10 h, the necrosis of the seminiferous epithelium is usually complete and irreversible. With incomplete occlusion, necrosis may be delayed. Torsion that lasts less than 6 h probably will not cause a testicular infarct. If torsion lasts longer than 24 h, the test is almost certainly will infarct [60, 61]. Although exceedingly rare, testicular torsion can be asynchronously bilateral [71].

The condition may be acute (symptoms last less than 6 weeks) or chronic (more than 3 months). Acute epididymitis is almost always unilateral. Gram-negative bacilli commonly cause acute epididymitis in children or following urinary tract instrumentation. The epididymis is sometimes the site of metastatic infection, such as tuberculosis.

7.4.6.2 Diagnosis

Testicular torsion results in acute pain and ischemia. The most common signs and symptoms include red, swollen scrotum, and acutely painful testicle, often in the absence of trauma. Nausea and vomiting are common. The most common conditions in the differential diagnosis include epididymitis, strangulated inguinal hernia, traumatic hematoma, testicular tumor, or testicular fracture. Physical examination techniques such

as scrotal elevation can help differentiate between epididymitis and testicular torsion. However, clinical examination of the scrotum is difficult due to the small size of the testes and the epididymis in infants and young children, and eliciting patients' history is challenging. Epididymitis has been considered uncommon in childhood, but its frequency has increased among children admitted with acute scrotum diagnosis [72].

The long-term prognosis for a functional, nonatrophied testicle is improved the sooner the torsion is diagnosed and treated. Therefore, confirming the diagnosis and quick management is crucial. Accordingly, imaging of the scrotum in children suspected of having the condition bears great importance [73, 74].

7.4.6.3 Scrotal Imaging

The classification of scrotal disorders in children into three typical clinical manifestations, namely acute scrotal disorders, scrotal masses, and cryptorchidism, is a helpful and practical basis for choosing the most suitable imaging modality available and commonly used modalities. These include sonography, scintigraphy, and magnetic resonance (MR) imaging. Either scintigraphy or sonography may be used as the first imaging study, and both can help distinguish among the disorders to different degrees. Although sonography provides superior anatomic details to scintigraphy, it may not be as accurate as it is thought to diagnose the most serious emergency reason for scrotal pain [74]. Scrotal masses are also best depicted with sonography with MRI as an adjunctive modality. In suspected cryptorchidism with equivocal clinical findings, both sonography and MR imaging are useful, but sonography is usually the initial study [75].

This strategy for imaging for acute scrotal disorders most relevant to nuclear medicine is not uniform and varies between the institutions based on the experience. In most institutions, Doppler ultrasound is used most commonly as the standard imaging technique of choice to confirm the diagnosis in most cases.

7.4.6.4 Scrotal Scintigraphy

Scintigraphy is used when color Doppler is inadequate, the diagnosis remains unclear, or if complications occur during the course of the disease. Radionuclide testicular scintigraphy is also used more commonly after the acute phase of the first 12 h, and vascular compromise has prolonged [76–78]. Recent studies comparing both modalities indicate similar sensitivity; the two studies may provide complementary information in indeterminate cases [79–81].

A study on 41 boys with suspected testicular torsion scintigraphy and Doppler ultrasound were performed and compared. There was no statistically significant difference in the sensitivity of both modalities. Specificity was 77% for color Doppler US and 97% for scintigraphy ($P = 0.05$). Due to the higher specificity, scintigraphy can help avoid unnecessary surgery when color Doppler US shows equivocal flow [81]. In another two studies of 21 and 37 patients, respectively, scintigraphy was more accurate than Doppler ultrasonography. It also has the advantage of being simple, fast, and accurate but without any detrimental effect on the human body [80, 82].

Findings on a normal scan are symmetrical perfusion with little uptake in the blood pool images. In acute torsion (early), there will be decreased perfusion on flow images, and the blood pool images will show no activity in the affected side (Fig. 7.11).

In missed torsion (late), there will be a halo of activity surrounding the torsion (a doughnut shape) due to increased perfusion to the surrounding tissue through the pudendal vessels (Fig. 7.12). There will be increased perfusion and hyperemia in acute epididymitis in the affected side due to vascular changes associated with the inflammation (Fig. 7.13) [83].

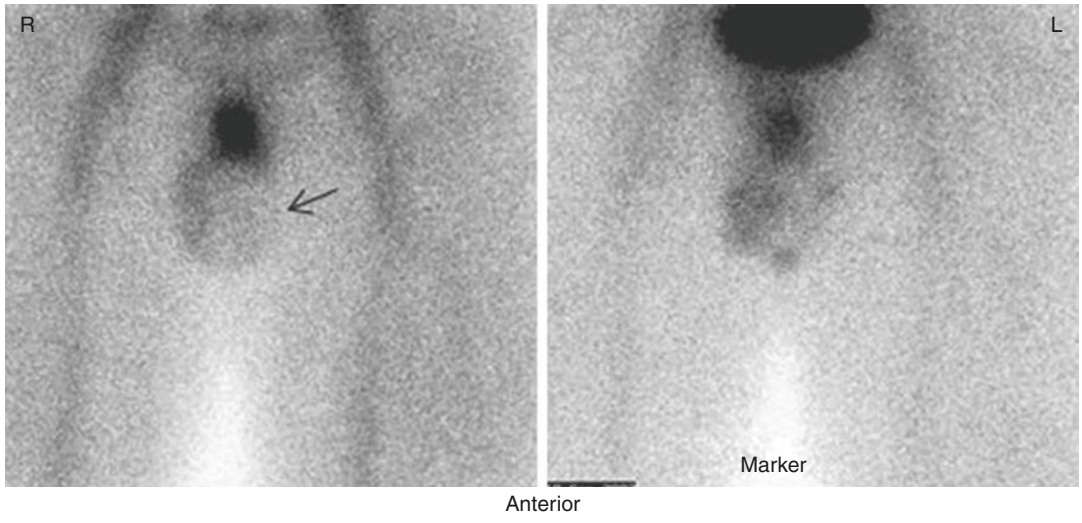

Fig. 7.11 99mTc-pertechnetate scrotal scan of a patient with acute scrotal pain in the left side. The study shows (**a**) essentially absent activity in the region of the left hemi-scrotum (arrow) corresponding to the left testicle by palpation markers (**b**). This case illustrates a pattern of acute testicular torsion

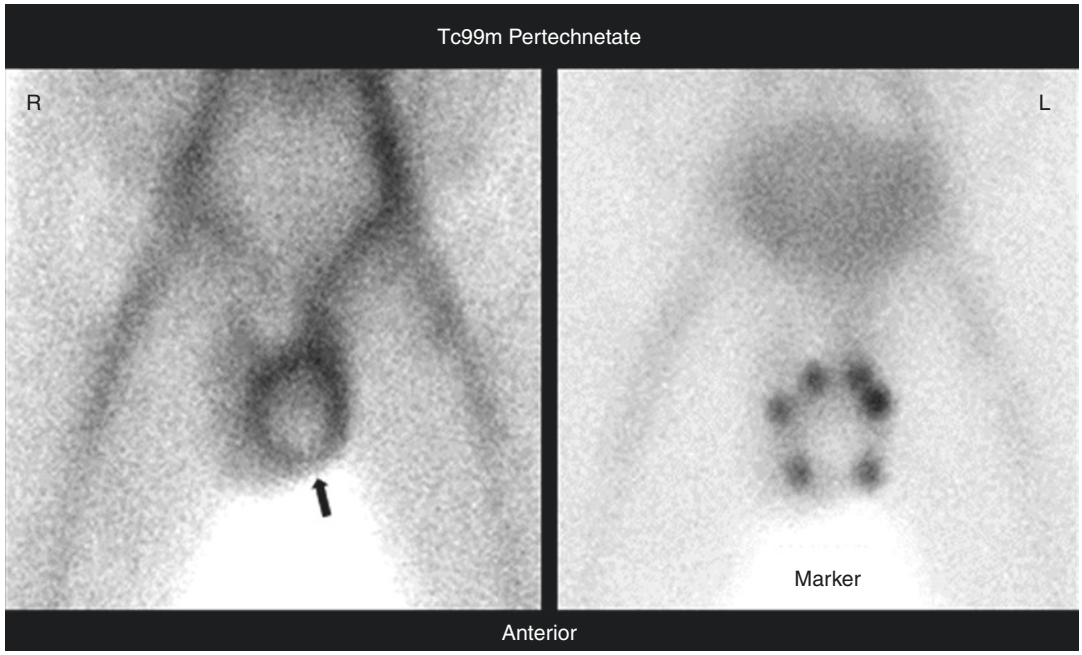

Fig. 7.12 99mTc-pertechnetate testicular imaging study showing the rim of increased uptake around the area of decreased uptake, illustrating the classic pattern of missed torsion of the left testis (arrow)

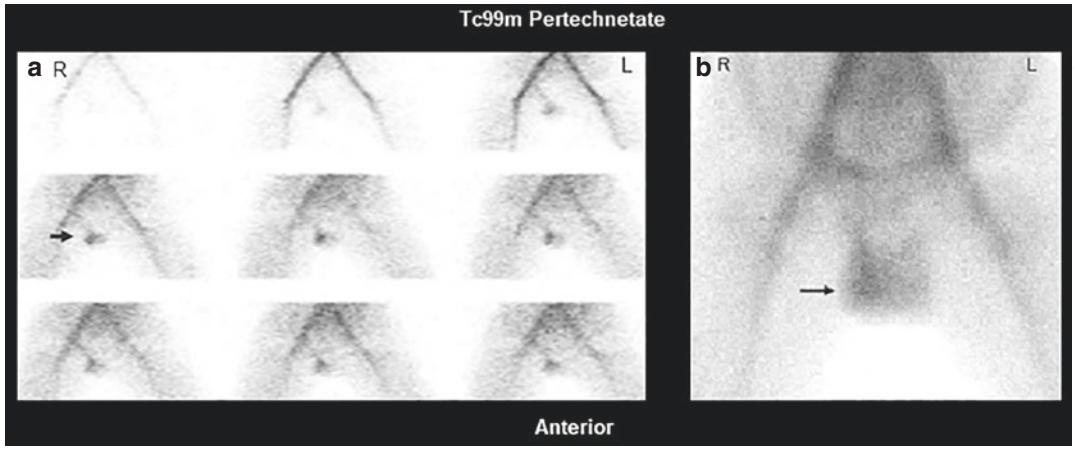

Fig. 7.13 A 14-year-old male was referred for a testicular scan to rule-out testicular torsion. The patient presented with 4 h-history of right-sided acute testicular pain and swelling. The pain was dull in nature, with no radiation, and was associated with nausea and vomiting. There was no history of fever or any urinary symptoms. The patient denied any history of trauma. On examination: Temperature was 37.4 °C. Left testis was grossly normal, and the right testis was tender and swollen. Lab investigations showed leukocytosis at 14,400. Testicular scan was performed, using l7-mCi Tc-99m Pertechnetate given äs a bolus intravenous injection. The scan shows increased flow (**a**) and blood pool (**b**) activity in the right hemiscrotum (arrows) in comparison to the left testis, indicating an inflammatory process in the right hemi-scrotum consistent with right epididymitis

References

1. Field M, Harris D, Pollock C (2010) 5-Glomerular filtration and acute kidney injury. In: Field M, Pollock C, Harris D (eds) The renal system, 2nd edn. Elsevier, pp 57–67
2. Chang A, Laszik ZG (2020) The kidney. In: Robbins pathologic basis of disease, 10th edn. WB Saunders Company
3. Chung AA, Millner PR (2020) Accessory renal artery stenosis and secondary hypertension. Case Rep Nephrol 2020:8879165. https://doi.org/10.1155/2020/8879165
4. Eshima D, Fritzberg AR, Taylor A Jr (1990) 99mTc renal tubular function agents: current status. Semin Nucl Med 20(1):28–40. https://doi.org/10.1016/s0001-2998(05)80174-6
5. Blaufox MD (1991) Procedures of choice in renal nuclear medicine. J Nucl Med 32(6):1301–1309
6. Rutland MD (1985) A comprehensive analysis of renal DTPA studies. I. Theory and normal values. Nucl Med Commun 6(1):11–20. https://doi.org/10.1097/00006231-198501000-00003
7. Jafri RA, Britton KE, Nimmon CC, Solanki K, Al-Nahhas A, Bomanji J, Fettich J, Hawkins LA (1988) Technetium-99m MAG3, a comparison with iodine-123 and iodine-131 orthoiodohippurate, in patients with renal disorders. J Nucl Med 29(2):147–158
8. Stabin M, Taylor A Jr, Eshima D, Wooter W (1992) Radiation dosimetry for technetium-99m-MAG3, technetium-99m-DTPA, and iodine-131-OIH based on human biodistribution studies. J Nucl Med 33(1):33–40
9. Raber SA, Schraml FV, Silverman ED (1997) Renal cortical retention of Tc-99m MAG3 in hypertension. Clin Nucl Med 22(3):190–192. https://doi.org/10.1097/00003072-199703000-00016
10. Levey CS, Schraml FV, Abreu SH, Silverman ED (1999) False-positive result of a captopril-enhanced radionuclide renogram in a child secondary to dehydration. Clin Nucl Med 24(1):6–8. https://doi.org/10.1097/00003072-199901000-00002
11. Taylor A Jr, Nally JV (1995) Clinical applications of renal scintigraphy. Am J Roentgenol 164(1):31–41. https://doi.org/10.2214/ajr.164.1.7998566
12. El-Maghraby TA, de Fijter JW, van Eck-Smit BL, Zwinderman AH, El-Haddad SI, Pauwels EK (1998) Renographic indices for evaluation of changes in graft function. Eur J Nucl Med 25(11):1575–1586. https://doi.org/10.1007/s002590050338
13. Olin JW, Piedmonte MR, Young JR, DeAnna S, Grubb M, Childs MB (1995) The utility of duplex ultrasound scanning of the renal arteries for diagnosing significant renal artery stenosis. Ann Intern Med 122(11):833–838. https://doi.org/10.7326/0003-4819-122-11-199506010-00004
14. Chrysochou C, Kalra PA (2009) Epidemiology and natural history of atherosclerotic renovascular disease. Prog Cardiovasc Dis 52(3):184–195. https://doi.org/10.1016/j.pcad.2009.09.001

15. Noilhan C, Barigou M, Bieler L, Amar J, Chamontin B, Bouhanick B (2016) Causes of secondary hypertension in the young population: a monocentric study. Ann Cardiol d'angeiol 65(3):159–164. https://doi.org/10.1016/j.ancard.2016.04.016
16. Safian RD, Textor SC (2001) Renal-artery stenosis. N Engl J Med 344(6):431–442. https://doi.org/10.1056/NEJM200102083440607
17. Martinez-Maldonado M (1991) Pathophysiology of renovascular hypertension. Hypertension 17(5):707–719. https://doi.org/10.1161/01.hyp.17.5.707
18. Sparks MA, Crowley SD, Gurley SB, Mirotsou M, Coffman TM (2014) Classical renin-angiotensin system in kidney physiology. Compr Physiol 4(3):1201–1228. https://doi.org/10.1002/cphy.c130040
19. Herrmann SM, Textor SC (2019) Renovascular hypertension. Endocrinol Metab Clin N Am 48(4):765–778. https://doi.org/10.1016/j.ecl.2019.08.007
20. Fine EJ, Sarkar S (1989) Differential diagnosis and management of renovascular hypertension through nuclear medicine techniques. Semin Nucl Med 19(2):101–115. https://doi.org/10.1016/s0001-2998(89)80005-4
21. Hricik DE, Browning PJ, Kopelman R, Goorno WE, Madias NE, Dzau VJ (1983) Captopril-induced functional renal insufficiency in patients with bilateral renal-artery stenoses or renal-artery stenosis in a solitary kidney. N Engl J Med 308(7):373–376. https://doi.org/10.1056/NEJM198302173080706
22. Blaufox MD, De Palma D, Taylor A, Szabo Z, Prigent A, Samal M, Li Y, Santos A, Testanera G, Tulchinsky M (2018) The SNMMI and EANM practice guideline for renal scintigraphy in adults. Eur J Nucl Med Mol Imaging 45(12):2218–2228. https://doi.org/10.1007/s00259-018-4129-6
23. Picciotto G, Sargiotto A, Petrarulo M, Rabbia C, De Filippi PG, Roccatello D (2003) Reliability of captopril renography in patients under chronic therapy with angiotensin II (AT1) receptor antagonists. J Nucl Med 44(10):1574–1581
24. Fommei E, Ghione S, Hilson AJ, Mezzasalma L, Oei HY, Piepsz A, Volterrani D (1993) Captopril radionuclide test in renovascular hypertension: a European multicentre study. European multicentre study group. Eur J Nucl Med 20(7):617–623. https://doi.org/10.1007/BF00176558
25. Taylor A, Nally J, Aurell M, Blaufox D, Dondi M, Dubovsky E, Fine E, Fommei E, Geyskes G, Granerus G, Kahn D, Morton K, Oei HY, Russell C, Sfakianakis G, Fletcher J (1996) Consensus report on ACE inhibitor renography for detecting renovascular hypertension. Radionuclides in Nephrourology Group. Consensus group on ACEI renography. J Nucl Med 37(11):1876–1882
26. Prigent A, Cosgriff P, Gates GF, Granerus G, Fine EJ, Itoh K, Peters M, Piepsz A, Rehling M, Rutland M, Taylor A Jr (1999) Consensus report on quality control of quantitative measurements of renal function obtained from the renogram: international consensus committee from the scientific committee of radionuclides in nephrourology. Semin Nucl Med 29(2):146–159. https://doi.org/10.1016/s0001-2998(99)80005-1
27. Mustafa S, Elgazzar AH (2013) Effect of the NSAID diclofenac on 99mTc-MAG3 and 99mTc-DTPA renography. J Nucl Med 54(5):801–806. https://doi.org/10.2967/jnumed.112.109595
28. Ludwig V, Martin WH, Delbeke D (2003) Calcium channel blockers: a potential cause of false-positive captopril renography. Clin Nucl Med 28(2):108–112. https://doi.org/10.1097/01.RLU.0000048679.45832.F3
29. Sarkar SD (1992) Diuretic renography: concepts and controversies. Urol Radiol 14(2):79–84. https://doi.org/10.1007/BF02926908
30. Fine EJ (1999) Interventions in renal scintirenography. Semin Nucl Med 29(2):128–145. https://doi.org/10.1016/s0001-2998(99)80004-x
31. Pohl HG, Rushton HG, Park JS, Belman AB, Majd M (2001) Early diuresis renogram findings predict success following pyeloplasty. J Urol 165(6 Pt 2):2311–2315. https://doi.org/10.1097/00005392-200106001-00024
32. Heyman S (1994) Radionuclide studies of the genitourinary tract. In: Miller J, Gelfand M (eds) Pediatric nuclear imaging. Saunders, Philadelphia, pp 195–211
33. Taylor AT, Brandon DC, de Palma D, Blaufox MD, Durand E, Erbas B, Grant SF, Hilson A, Morsing A (2018) SNMMI procedure standard/EANM practice guideline for diuretic renal scintigraphy in adults with suspected upper urinary tract obstruction 1.0. Semin Nucl Med 48(4):377–390. https://doi.org/10.1053/j.semnuclmed.2018.02.010
34. Ring P, Huether SE (2017) Alteration of renal and urinary tract function in children. In: McCance KL, Huether SE (eds) Pathophysiology, 8th edn. Mosby, Philadelphia, pp 1278–1295
35. Strand WR (1999) Urinary infection in children: pathogenesis, bacterial virulence, and host resistance. In: Bauer SB, Gonzales E (eds) Pediatric urology practice. Lippincott Williams & Wilkins, Philadelphia, pp 433–461
36. Kaefer M, Diamond D (1987) Vesicoureteral reflux. In: Retik A, Cukier J (eds) Pediatric urology. Williams and Wilkins, Baltimore, pp 463–486
37. Solari V, Owen D, Puri P (2005) Association of transforming growth factor-beta1 gene polymorphism with reflux nephropathy. J Urol 174(4 Pt 2):1609–1611. https://doi.org/10.1097/01.ju.0000179385.64585.dc
38. Kanematsu A, Yamamoto S, Yoshino K, Ishitoya S, Terai A, Sugita Y, Ogawa O, Tanikaze S (2005) Renal scarring is associated with nonsecretion of blood type antigen in children with primary vesicoureteral reflux. J Urol 174(4 Pt 2):1594–1597. https://doi.org/10.1097/01.ju.0000176598.60310.90
39. Shaikh N, Osio VA, Wessel CB, Jeong JH (2020) Prevalence of asymptomatic bacteriuria in children: a meta-analysis. J Pediatr 217:110–117.e4. https://doi.org/10.1016/j.jpeds.2019.10.019
40. Mahyar A, Ayazi P, Mavadati S, Oveisi S, Habibi M, Esmaeily S (2014) Are clinical, laboratory, and

imaging markers suitable predictors of vesicoureteral reflux in children with their first febrile urinary tract infection? Korean J Urol 55(8):536–541. https://doi.org/10.4111/kju.2014.55.8.536
41. Subcommittee on urinary tract infection (2016) Reaffirmation of AAP clinical practice guideline: the diagnosis and management of the initial urinary tract infection in febrile infants and young children 2-24 months of age. Pediatrics 138(6):e20163026. https://doi.org/10.1542/peds.2016-3026
42. National Institute for Health and Clinical Excellence (NICE) (2018) Clinical guideline 54—Urinary tract infection in under 16s: diagnosis and management. Clinical guideline Published: 22 August 2007. www.nice.org.uk/guidance/cg54
43. Pokrajac D, Sefic-Pasic I, Begic A (2018) Vesicoureteral reflux and renal scarring in infants after the first febrile urinary tract infection. Med Archiv 72(4):272–275. https://doi.org/10.5455/medarh.2018.72.272-275
44. Roupakias S, Sinopidis X, Tsikopoulos G, Spyridakis I, Karatza A, Varvarigou A (2017) Dimercaptosuccinic acid scan challenges in childhood urinary tract infection, vesicoureteral reflux and renal scarring investigation and management. Minerva Urol Nefrol 69(2):144–152. https://doi.org/10.23736/S0393-2249.16.02509-1. Epub 2016 Jun 29. PMID: 27355216
45. Breinbjerg A, Jørgensen CS, Frøkiær J et al (2021) Risk factors for kidney scarring and vesicoureteral reflux in 421 children after their first acute pyelonephritis, and appraisal of international guidelines. Pediatr Nephrol 36(9):2777–2787
46. Ramos CD, Onusic DM, Brunetto SQ, Amorim BJ, Souza TF, Saad S, Lima M (2019) Technetium-99m-dimercaptosuccinic acid renal scintigraphy and single photon emission computed tomography/computed tomography in patients with sickle cell disease. Nucl Med Commun 40(11):1158–1165. https://doi.org/10.1097/MNM.0000000000001086
47. Vasco M, Benincasa G, Fiorito C, Faenza M, De Rosa P, Maiello C, Santangelo M, Vennarecci G, Napoli C (2021) Clinical epigenetics and acute/chronic rejection in solid organ transplantation: an update. Transplant Rev 35(2):100609. https://doi.org/10.1016/j.trre.2021.100609
48. Hruba P, Madill-Thomsen K, Mackova M, Klema J, Maluskova J, Voska L, Parikova A, Slatinska J, Halloran PF, Viklicky O (2020) Molecular patterns of isolated tubulitis differ from tubulitis with interstitial inflammation in early indication biopsies of kidney allografts. Sci Rep 10(1):22220
49. Callemeyn J, Ameye H, Lerut E, Senev A, Coemans M, Van Loon E, Sprangers B, Van Sandt V, Rabeyrin M, Dubois V, Thaunat O, Kuypers D, Emonds MP, Naesens M (2020) Revisiting the changes in the Banff classification for antibody-mediated rejection after kidney transplantation. Am J Transplant 21(7):2413–2423. https://doi.org/10.1111/ajt.16474
50. Randhawa PS, Tsamandas AC, Magnone M, Jordan M, Shapiro R, Starzl TE, Demetris AJ (1996) Microvascular changes in renal allografts associated with FK506 (Tacrolimus) therapy. Am J Surg Pathol 20(3):306–312. https://doi.org/10.1097/00000478-199603000-00007
51. Asher J, Vasdev N, Wyrley-Birch H, Wilson C, Soomro N, Rix D, Jaques B, Manas D, Torpey N, Talbot D (2014) A prospective randomised paired trial of sirolimus versus tacrolimus as primary immunosuppression following non-heart beating donor kidney transplantation. Curr Urol 7(4):174–180. https://doi.org/10.1159/000365671
52. Munib S, Ahmed T, Ahmed R, Najam-Ud-Din (2021) Renal allograft biopsy findings in live-related renal transplant recipients. J College Physic Surg 31(2):197–201. https://doi.org/10.29271/jcpsp.2021.02.197
53. Lebowitz RL, Olbing H, Parkkulainen KV, Smellie JM, Tamminen-Möbius TE (1985) International system of radiographic grading of vesicoureteric reflux. International reflux study in children. Pediatr Radiol 15(2):105–109. https://doi.org/10.1007/BF02388714
54. Williams G, Fletcher JT, Alexander SI, Craig JC (2008) Vesicoureteral reflux. J Am Soc Nephrol 19(5):847–862. https://doi.org/10.1681/ASN.2007020245
55. Rodriguez MM (2004) Developmental renal pathology: its past, present, and future. Fetal Pediatr Pathol 23(4):211–229. https://doi.org/10.1080/15227950490923453
56. Jana S, Blaufox MD (2006) Nuclear medicine studies of the prostate, testes, and bladder. Semin Nucl Med 36(1):51–72. https://doi.org/10.1053/j.semnuclmed.2005.09.001
57. Kopac M, Kenig A, Kljucevsek D, Kenda RB (2005) Indirect voiding urosonography for detecting vesicoureteral reflux in children. Pediatr Nephrol 20(9):1285–1287. https://doi.org/10.1007/s00467-005-1961-2
58. Charbonneau SG, Tackett LD, Gray EH, Caesar RE, Caldamone AA (2005) Is long-term sonographic followup necessary after uncomplicated ureteral reimplantation in children? J Urol 174(4 Pt 1):1429–1432. https://doi.org/10.1097/01.ju.0000173128.73742.bc
59. Giel DW, Noe HN, Williams MA (2005) Ultrasound screening of asymptomatic siblings of children with vesicoureteral reflux: a long-term followup study. J Urol 174(4 Pt 2):1602–1605. https://doi.org/10.1097/01.ju.0000176596.87624.a3
60. Penido Silva JM, Oliveira EA, Diniz JS, Bouzada MC, Vergara RM, Souza BC (2006) Clinical course of prenatally detected primary vesicoureteral reflux. Pediatr Nephrol 21(1):86–91. https://doi.org/10.1007/s00467-005-2058-7
61. Muschat M (1932) The pathological anatomy of testicular torsion: explanation of its mechanism. Surg Gynaecol Obstet 54:758–763
62. Allan WR, Brown RB (1966) Torsion of the testis: a review of 58 cases. Br Med J 1(5500):1396–1397. https://doi.org/10.1136/bmj.1.5500.1396

63. Scorer CG, Farrington GH (1971) Congenital deformities of testis and epididymis, 1st edn. Butterworth, London
64. Corriere JN Jr (1972) Horizontal lie of the testicle: a diagnostic sign in torsion of the testis. J Urol 107(4):616–617. https://doi.org/10.1016/s0022-5347(17)61093-0
65. Skoglund RW, McRoberts JW, Ragde H (1970) Torsion of testicular appendages: presentation of 43 new cases and a collective review. J Urol 104(4):598–600. https://doi.org/10.1016/s0022-5347(17)61790-7
66. Rencken RK, du Plessis DJ, de Haas LS (1990) Venous infarction of the testis—a cause of non-response to conservative therapy in epididymo-orchitis. A case report. S Afr Med J 78(6):337–338
67. Kogan SJ (2002) Swellings of the intrascrotal contents. In: Gillenwalter JY (ed) Adult and pediatric urology, 4th edn. Lippincott Williams & Wilkins, Philadilphia
68. Frush DP, Babcock DS, Lewis AG, Paltiel HJ, Rupich R, Bove KE, Sheldon CA (1995) Comparison of color Doppler sonography and radionuclide imaging in different degrees of torsion in rabbit testes. Acad Radiol 2(11):945–951. https://doi.org/10.1016/s1076-6332(05)80693-2
69. Luker GD, Siegel MJ (1994) Color Doppler sonography of the scrotum in children. Am J Roentgenol 163(3):649–655. https://doi.org/10.2214/ajr.163.3.8079863
70. Herbener TE (1996) Ultrasound in the assessment of the acute scrotum. J Clin Ultrasound 24(8):405–421. https://doi.org/10.1002/(SICI)1097-0096(199610)24:8<405::AID-JCU2>3.0.CO;2-O
71. Patriquin HB, Yazbeck S, Trinh B, Jéquier S, Burns PN, Grignon A, Filiatrault D, Garel L, Dubois J (1993) Testicular torsion in infants and children: diagnosis with Doppler sonography. Radiology 188(3):781–785. https://doi.org/10.1148/radiology.188.3.8351347
72. Olguner M, Akgür FM, Aktuğ T, Derebek E (2000) Bilateral asynchronous perinatal testicular torsion: a case report. J Pediatr Surg 35(9):1348–1349. https://doi.org/10.1053/jpsu.2000.9330
73. Pogorelić Z, Mustapić K, Jukić M, Todorić J, Mrklić I, Mešštrović J, Jurić I, Furlan D (2016) Management of acute scrotum in children: a 25-year single center experience on 558 pediatric patients. Can J Urol 23(6):8594–8601
74. Laher A, Ragavan S, Mehta P, Adam A (2020) Testicular torsion in the emergency room: a review of detection and management strategies. Open Access Emerg Med 12:237–246. https://doi.org/10.2147/OAEM.S236767
75. Hörmann M, Balassy C, Philipp MO, Pumberger W (2004) Imaging of the scrotum in children. Eur Radiol 14(6):974–983. https://doi.org/10.1007/s00330-004-2248-x
76. Shin J, Jeon GW (2020) Comparison of diagnostic and treatment guidelines for undescended testis. Clin Exp Pediatr 63(11):415–421. https://doi.org/10.3345/cep.2019.01438
77. Lavallee ME, Cash J (2005) Testicular torsion: evaluation and management. Curr Sports Med Rep 4(2):102–104. https://doi.org/10.1097/01.csmr.0000306081.13064.a2
78. Ring N, Staatz G (2017) Bildgebende Diagnostik beim akuten Skrotum [Diagnostic imaging in cases of acute scrotum]. Aktuelle Urol 48(5):443–451. https://doi.org/10.1055/s-0043-100497
79. Saleh O, El-Sharkawi MS, Imran MB (2012) Scrotal scintigraphy in testicular torsion: an experience at a tertiary care centre. IIUM Med J Malaysia 11(1). https://doi.org/10.31436/imjm.v11i1.540
80. Yuan Z, Luo Q, Chen L, Zhu J, Zhu R (2001) Clinical study of scrotum scintigraphy in 49 patients with acute scrotal pain: a comparison with ultrasonography. Ann Nucl Med 15(3):225–229. https://doi.org/10.1007/BF02987836
81. Nussbaum Blask AR, Bulas D, Shalaby-Rana E, Rushton G, Shao C, Majd M (2002) Color Doppler sonography and scintigraphy of the testis: a prospective, comparative analysis in children with acute scrotal pain. Pediatr Emerg Care 18(2):67–71. https://doi.org/10.1097/00006565-200204000-00001
82. Wu HC, Sun SS, Kao A, Chuang FJ, Lin CC, Lee CC (2002) Comparison of radionuclide imaging and ultrasonography in the differentiation of acute testicular torsion and inflammatory testicular disease. Clin Nucl Med 27(7):490–493. https://doi.org/10.1097/00003072-200207000-00005
83. Saha GB (2010) Fundamentals of nuclear pharmacy, 6th edn. Springer, Berlin